Chem Soc Rev

Knot Theory in Modern Chemistry

Journal:	*Chemical Society Reviews*
Manuscript ID	CS-TRV-06-2016-000448.R1
Article Type:	Tutorial Review
Date Submitted by the Author:	10-Aug-2016
Complete List of Authors:	Horner, Kate; Durham University, Department of Mathematical Sciences Miller, Mark; Durham University, Department of Chemistry Steed, Jonathan; Durham University, Department of Chemistry Sutcliffe, Paul; Durham University, Department of Mathematical Sciences

Journal Name

RSCPublishing

ARTICLE

Knot Theory in Modern Chemistry

Cite this: DOI: 10.1039/xoxxoooooox

Kate E. Horner,*[a] Mark A. Miller,[b] Jonathan W. Steed[b] and Paul M. Sutcliffe[a]

Received ooth January 2012,
Accepted ooth January 2012

DOI: 10.1039/xoxxoooooox

www.rsc.org/

Knot theory is a branch of pure mathematics, but it is increasingly being applied in a variety of sciences. Knots appear in chemistry, not only in synthetic molecular design, but also in an array of materials and media, including some not traditionally associated with knots. Mathematics and chemistry can now be used synergistically to identify, characterise and create knots, as well as to understand and predict their physical properties. This tutorial review provides a brief introduction to the mathematics of knots and related topological concepts in the context of the chemical sciences. We then survey the broad range of applications of the theory to contemporary research in the field.

Key Learning Points

- Some fundamentals of knot theory.
- Knot theory and closely related ideas in topology can be applied to modern chemistry.
- Knots can be formed in single molecules as well as in materials and biological fibres using a mixture of self-assembly, metal templating and optical manipulation.
- The inclusion of knots in molecular structures can alter chemical and physical properties.
- Knots are surprisingly ubiquitous in the chemical sciences.

1. Introduction to Knot Theory

The birth of mathematical knot theory can be traced back to the work of Vandermonde (1771),[1] who was a musician by training, but in later life made contributions to both mathematics and chemistry. However, it was physicists of the mid-19th century who provided the impetus for the development of modern knot theory, which today is an area of mathematics within the field of topology. In 1867, Sir William Thomson (later to become Lord Kelvin) proposed that atoms are composed of knotted vortices of the aether.[2] While this hypothesis subsequently turned out to be incorrect, not least because the existence of the aether was later disproved, it did spark a fascination with knots that has lasted for well over a century. In mathematical terms, a knot is defined as a non-self-intersecting closed curve in three-dimensional space. Importantly, this means that for a knot in a piece of rope to be considered a mathematical knot, the free ends must be joined. On a closed loop, the knot can be distorted but not removed or fundamentally altered.

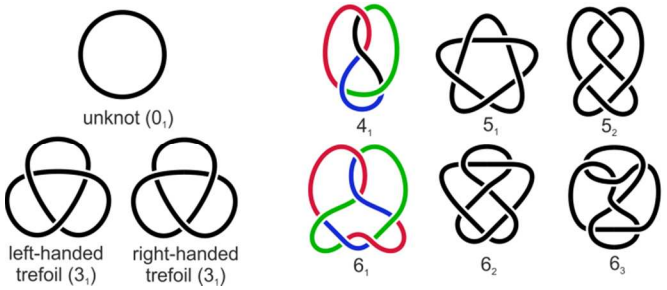

Figure 1: A selection of knot diagrams showing some of the simplest knots. The knots are labelled with Alexander-Briggs notation, where the main number denotes the crossing number and the subscript enumerates knots with the same crossing number. The order has no real significance. The 6_1 knot is shown in its tricoloured form (see text). The black strand in the 4_1 knot cannot be assigned to red, green or blue within the rules of tricolourability.

The theory of abstract mathematical knots is concerned with the characteristics that are locked into a closed curve by the presence of a given knot. These characteristics allow knots to be classified and compared, and provide a basis for understanding the implications of knots when they arise in a physical system. Knots are being found to play a role in more and more scientific contexts, and knot theory is therefore gradually making its way into many fields of study, from chemistry to physics and even anthropology.[3]

In this tutorial review we examine the application of knot theory broadly across the chemical sciences, ranging from its direct application to molecular and colloidal structures, to less clear-cut systems such as tangled gel matrices, knotted proteins, and interwoven polymers. In mature areas that have been previously reviewed in more depth, such as molecular and biological knots, we include just fundamental points, a few recent developments and key references to more specialised reviews. For more detail on the underlying theory of knots outlined in this article, we recommend the highly accessible introductory text by Adams.[3]

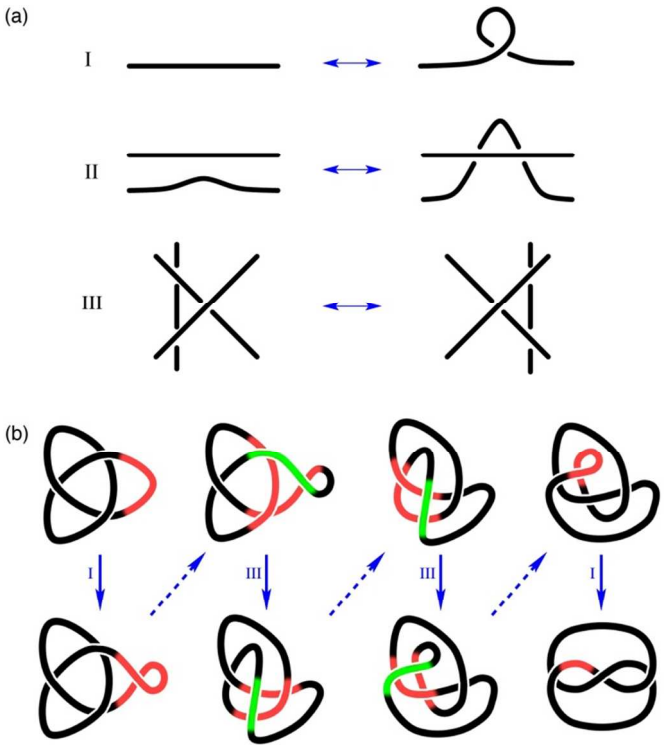

Figure 2: a) Reidemeister moves I to III for interconverting knot diagrams. Each move has an analogous version where overcrossings and undercrossings are interchanged. b) The deformation of the traditional three-lobed diagram of the trefoil knot (top left) into the isomorphic but less familiar two-lobed diagram (bottom right) by a sequence of four Reidemeister moves. In each step, the region of the diagram that is being manipulated has been highlighted in colour.

1.1 Classification of Knots

An important aspect of knot theory is the classification of knots, which is designed to answer questions like: What kind of knot is this? Are these two knots the same? Is this the simplest way to draw this knot? Is this knot actually just the unknot? The unknot (see Figure 1), also called the trivial knot, is simply a closed curve which can be smoothly deformed into a circle. It is necessary to include the unknot in knot theory for completeness; defining the unknot is analogous to including zero in the set of integers, so that when counting objects we are able to deal with the case of not having any objects at all.

Two knots are considered to be the same if one can be smoothly deformed into the other, whilst avoiding self-intersections. To draw a knot, it is convenient to project the curve in three-dimensional space onto a plane, to produce a knot diagram (some examples are displayed in Figure 1) consisting of strands with crossings, where the strand that goes under must be distinguished from the strand that goes over. For a given knot, different knot diagrams can be obtained by changing the plane of the projection. Furthermore, smooth deformations that keep the knot topologically the same may change the number of crossings in an associated knot diagram. Any two diagrams of the same knot can be interconverted by a suitable sequence of just three types of elementary "Reidemeister moves", shown in Figure 2. For example, the interconversion of two equally valid representations of the trefoil knot by two Reidemeister moves of type I and two of type III is shown in Figure 2b.

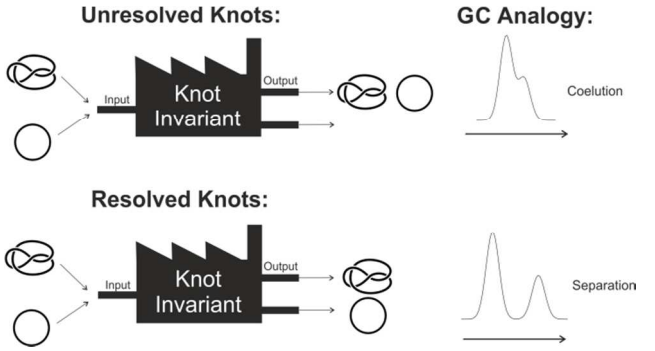

Figure 3: Schematic of output from successful and unsuccessful knot invariants for distinguishing knots. A knot invariant which does not successfully distinguish two different knots is analogous with failed separation in gas chromatography (GC) resulting in coelution.

Reidemeister moves of type I and II change the number of crossings in a diagram. A suitable sequence of all three types of Reidemeister moves can therefore (in principle) be used to simplify a given knot diagram until the number of crossings can be reduced any further, and this number is then called the crossing number of the knot. The crossing number is useful in the taxonomy of knots. For example, the knots in Figure 1 are labelled according to their crossing number using Alexander-Briggs notation, where knots with the same crossing number are grouped together and labelled with a subscript (the order of labels for a given crossing number is arbitrary and so has no real significance).

Converting a knot diagram to its simplest form may be difficult in practice if there is a large number of crossings. Consequently, an important challenge in knot theory is to determine the knot to which a particular knot diagram corresponds. Key tools in this endeavour are knot invariants, which input a knot and output a mathematical object, for example a binary digit (True or False), an integer, a polynomial, or something more complicated. We have already seen one example of a knot invariant, namely the crossing number, where the output is an integer. The crucial property of a knot invariant is that any two diagrams of the same knot have identical values of the invariant. In other words, smooth deformations of a knot do not affect knot invariants. We see from Figure 1 that the unknot and the trefoil are not the same knot, as they have different values (zero and three respectively) for the invariant crossing number. On the other hand, the three knots in Figure 1 that have crossing number six cannot be distinguished on the basis of this invariant alone.

Some invariants output a polynomial, consisting of coefficients and powers of an arbitrary variable, t. For example, the so-called Alexander polynomial of the trefoil is $\Delta(t) = t - 1 + t^{-1}$. Knot polynomials are rather abstract objects; in most applications, the variable t has no physical significance and a plot of $\Delta(t)$ against t also lacks a simple interpretation. For the purpose of identifying knots, the important features of the polynomial are the powers of t that appear in it (1, 0 and -1 for the trefoil example) and their coefficients (1, -1 and 1). These

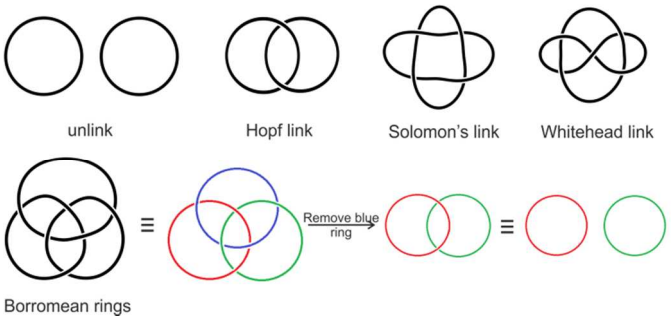

Figure 4: Some of the simplest links. The Hopf link, Solomon's link and Whitehead link are all two-component links while the Borromean rings are an example of a three-component link. The Borromean rings are also Brunnian which means that removal of any one component (in this figure, the blue ring) leaves the unlink.

powers and coefficients are determined by the order in which the over- and under-crossings of the knot are encountered as one moves along the curve and, crucially, the same set of powers and coefficients is obtained for any diagram of a given knot. Hence, the pattern of powers and coefficients of *t* are a "fingerprint" of a knot's topology regardless of how it is drawn. Identifying a knot from the powers and coefficients of its polynomial is analogous to the way that a chemist might identify a molecule from the fragmentation pattern in its mass spectrum.

Other common knot polynomials include the Jones and HOMFLY polynomials, which, like the Alexander polynomial, are named after their discoverers. The polynomials can be computed from a knot diagram and hence have an important role in answering the central question of whether two diagrams represent the same knot. However, the Alexander polynomial cannot distinguish between all the knots displayed in Figure 1, because the left-handed and right-handed trefoils have the same Alexander polynomial. The two versions of the trefoil are nevertheless distinct knots because one cannot be continuously deformed into the other. One way to tell the left- and right-handed trefoils apart is by their respective Jones polynomials, which (unlike the Alexander polynomials) do have different sets of coefficients and powers. Knots like these, which cannot be smoothly deformed into their own mirror image, are called topologically chiral. This concept of chirality is similar to that in chemistry, where a chiral molecule has a non-superimposable mirror image. However, it is important to remember that topological chirality is defined by the inability of a knot to be *deformed* into its mirror image, and not by the particular geometrical configuration of a knotted structure.

The Jones polynomial, and its HOMFLY generalisation, can distinguish between all the knots shown in Figure 1, including the mirror images of the trefoil, but for knots with ten or more crossings there are examples of different knots that have the same polynomial, even for some knots with different crossing numbers. In fact, it is still unknown whether there is a non-trivial knot that has the same Jones polynomial as the unknot. Despite these limitations, knot polynomials are still amongst the most useful tools for distinguishing between knots because they do distinguish many knots and can be systematically derived from a given knot diagram. Knot classification is still a daunting task, even for fairly small crossing numbers, as there are more than 1.7 million different knots with sixteen or fewer crossings. It is not known whether there exists a knot polynomial that is a complete invariant, *i.e.,* one that would uniquely identify all knots.

An analogy can be made between calculating a knot invariant and performing gas chromatography. In chromatography, the goal is complete separation of all chemical components and failure to achieve this results in co-elution (see Figure 3). This means that two different eluates could mistakenly be identified as being the same compound. The same is true of an incomplete knot invariant; a given invariant may be unable to distinguish between two knots that are actually different. An extreme example is a knot invariant that takes only the values True or False, such as tricolourability. A knot is tricolourable if each of the strands between adjacent undercrossings in a projection can be assigned one of three colours such that each crossing brings together either all three colours or just one colour (excluding the trivial possibility of assigning the same colour to all strands). For example, the 6_1 knot is tricolourable whereas 4_1 is not (see Figure 1). As this knot invariant separates all knots into only two types, it is clearly unable to identify a specific knot. However, it can, for example, distinguish between the trefoil knot and the unknot, since the former returns True and the latter False. Stronger knot invariants, such as knot polynomials, allow a better distinction between knots, and work effectively for all knots below a certain level of complexity.

1.2 Links

The concept of a knot can be extended to include collections of non-intersecting closed curves, which are known as links. A knot is then the special case of a link with only one component. Much of the treatment of knots, such as the polynomials, can be generalised to links. Just as the trivial knot is called the unknot, there are trivial links or "unlinks". The two-component unlink, which is just two distinct unknots, can be seen in Figure 4. The simplest non-trivial two-component link is the Hopf link, also displayed in Figure 4, where two unknots are linked once, as exemplified in chemical systems by [2]catenanes. The simplest link invariant is the number of components but another important invariant is the linking number, which is an integer that measures how many times each component winds round the other. It does this by counting the number of crossings between the strands of the two components, distinguishing between the two possible orientations of crossings, denoted positive and negative as illustrated in Figure 5. The linking number is half the difference between the number of positive and negative crossings. Reversing the orientation of either component changes the sign of the linking number, but its absolute value is independent of the choice of orientations. It is perhaps not surprising to find that (with appropriate choices of orientation) the unlink, Hopf link and Solomon's link, presented in Figure 4, have linking number 0, 1 and 2, respectively. It is less obvious that the Whitehead link, also shown in Figure 4, has linking

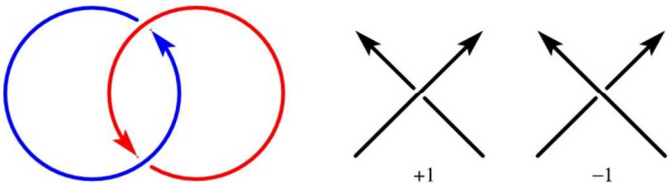

Figure 5: To calculate the linking number, each component must be assigned an orientation (left). A crossing with positive orientation is then one where the overstrand must be rotated anticlockwise to point in the same direction as the understrand, while negative orientation is the opposite. (For the orientations shown in the Hopf link above, both crossings are negative.)

number zero, but this is a result of it having an equal number of positive and negative crossings, yielding zero for the difference. Turning to non-trivial links with three or more components, an interesting family are the Brunnian links, which are defined by the property that the removal of any one component leaves only unlinked unknots. The Borromean rings (Figure 4) are the simplest example, and consist of three linked unknots, no pair of which are directly threaded through one another.

Just as for knots, Alexander-Briggs notation can be used for links by adding a superscript to show the number of components in the link. For example, the two-component unlink (shown in Figure 4) is denoted 0_1^2 while the Hopf link is 2_1^2 and the Solomon's link 4_1^2.

1.3 Möbius Strips

There is also an intrinsic connection between knot theory and the strange topology of Möbius strips. A physical Möbius strip can be formed by half-twisting a strip of paper an odd number of times and then fixing the ends together. This has the intriguing effect of giving the object only a single edge and a single side. With one half-twist, the edge forms the unknot but with three half-twists the edge forms the trefoil knot.

Certain characteristics of Möbius strips have been known in molecular systems for some time.[4] For example, Möbius aromaticity involves a twisted arrangement of the conjugated π orbitals and requires $4n$ π-electrons, in contrast to the more common Hückel aromaticity, which requires $4n + 2$ electrons. The difference in the aromaticity rule arises from the fact that an odd number of half-twists in the chain of p-π orbitals necessitates a mismatched, anti-bonding, overlap at some point in the chain. The mismatch is a manifestation of the fact that Möbius strips are non-orientable. This means that it is impossible to choose a unit normal vector consistently at all points on the surface (see Figure 6). In Section 5 we will see that the topological property of non-orentability can have important physical consequences.

1.4 Braids

There is an intimate relationship between knots, links and braids. A braid is a set of intertwined strings that are fixed at the top and bottom and are always pointing downwards, so that no string ever turns back up. This is like plaited hair, where the strands are fixed at the scalp and at the bottom by a hair band. Braids are inherently related to knot theory since all knots and links can be obtained as the closure of a braid by joining the ends (see Figure 7 for an example). However, the closure of different braids can produce the same link, just as different knot diagrams may correspond to the same knot. It is interesting to note that the Jones polynomial was originally defined as a braid invariant that was shown to depend only on the type of the closed braid.

2. Molecular Knots

Perhaps the most direct way to apply knot theory to chemistry is to synthesise molecules with knotted topology. An obvious starting point is a knot with the smallest crossing number. Creating a knotted topology using indirect chemical synthesis methods is a significant challenge and requires careful reaction design and the use of templating methods. The field is highly active and a wide range of creative techniques have been employed to produce knotted and linked molecules. Some key illustrative advances are summarised in Figure 8 (see References 5–7 for extensive reviews).

2.1 Simple Molecular Knots

Figure 6: A Möbius strip is non-orientable: it is impossible to make a consistent choice of normal vector at all points on the surface, as illustrated by the sudden change in direction of the drawing pins at the front of this photograph.

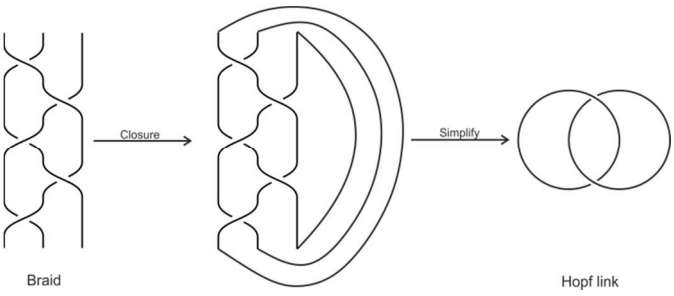

Figure 7: A three-string braid with fixed ends (left) and its closure (middle) obtained by joining the ends. The resulting link can be simplified to identify it as the Hopf link (right).

So far only three different knot types have been realised synthetically, namely the 3_1 trefoil knot, the 4_1 figure-of-eight knot and the 5_1 pentafoil knot.[7] The first well characterised molecular knot was a trefoil synthesised by Dietrich-Buchecker and Sauvage in 1989 (Figure 8a).[8] This landmark advancement was achieved by using transition metal templating to form a helical structure which was then covalently cyclised to create a permanent knot. Templating is an effective route to knot synthesis because metal ions have a well-defined coordination geometry and the strength of coordination strikes the right balance between lability and stability to promote reliable formation of the desired structure. It is also possible for the metal ions to serve a dual purpose by catalysing the ring closure chemistry that links the templated fragments.[6] Trefoil knots have also been produced by hydrogen-bonded templating methods, as in amide-amide hydrogen bonding and by dynamic combinatorial chemistry (DCC) approaches which have given rise to a trefoil knot reported by Sanders and co-workers in 2012 (Figure 8b) based on a naphthalenediimide aqueous disulfide dynamic combinatorial library. The knot assembly is driven by hydrophobic effects. DCC methods have also resulted in a figure-of-eight knot (Figure 8e) and Solomon's link reported in 2014.[6] Interestingly, resolved chiral building blocks give rise to a topologically achiral figure-of-eight knot while a racemic mixture gives a different *meso* figure-of-eight knot. A Solomon's link was also produced in 2013 by the Leigh group based on metal templating via a tetrameric cyclic double helicate scaffold (Figure 8f).[7]

For more complex knots, metal templating must be used alongside other self-assembly and synthetic techniques in order to obtain the desired structure rather than a complex mixture or unknotted products. This is the case for the more recently prepared molecular pentafoil knot (Figure 8c and the knot labelled 5_1 in Figure 1) which is the most complex, non-DNA molecular knot prepared to date.[9] Here, reversible metal-imine bond coordination was used to allow correction of any unwanted bond formation. Moreover, anion templating with chloride and careful use of stereoelectronic effects, symmetry and linker length, were all needed in order to form this complicated structure.

In very recent work,[10] the pentafoil knot has been reached by a different route, based on ring-closing olefin metathesis. This approach has the advantage that, once the knot has been formed, the Fe(II) template in each of the pentafoil's five lobes and the halide ion in its central cavity can be removed, leaving the uncoordinated knotted ligand. Without the metal cations, the ligand is flexible, but can readily be rigidified by coordination with Zn(II) ions in place of the original Fe(II). This metallated form acts as an effective catalyst for carbon-halogen bond cleavage because it is one of the strongest noncovalent binding synthetic hosts of Cl^- and Br^- known. It can efficiently catalyse the generation of a carbocation from the hydrolysis of bromodiphenylmethane for example, whereas the unknotted form is inactive. The knot structure is crucial in achieving this chemical function because it restricts the conformations that the ligand may adopt, stabilising the active form. The metal-free knotted ligand is catalytically inactive, providing a means for allosteric regulation of the catalysis; binding of metal ions at one set of locations (the lobes of the pentafoil) affects binding of the halide at another point (the central cavity).

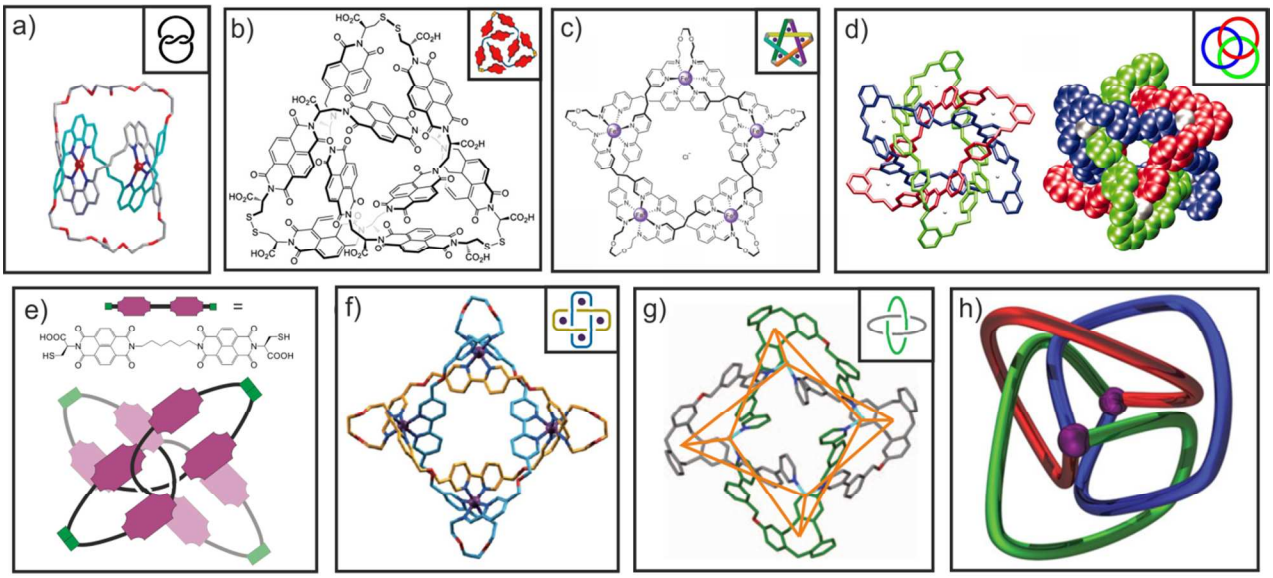

Figure 8: a) The first molecular trefoil knot (see Figure 2b for this representation of the trefoil), prepared by Sauvage using metal-templating. Adapted from Reference 6 with permission from the Royal Society of Chemistry. b) An organic trefoil knot prepared by Sanders and co-workers using DCC. Figure adapted from Reference 7. c) The first pentafoil knot, synthesised by Leigh and co-workers. Figure adapted with permission from Reference 9. d) Molecular Borromean Rings. Figure adapted with permission from Reference 19. e) Schematic of a molecular figure-of-eight knot synthesised by Sanders and co-workers.7 f) A Solomon Link. Figure adapted from Reference 7. g) A "Solomon Cube" by Ronson *et al.* Figure adapted with permission from Reference 17. h) Representation of the universal 3-ravel. Figure adapted with permission from Reference 23.

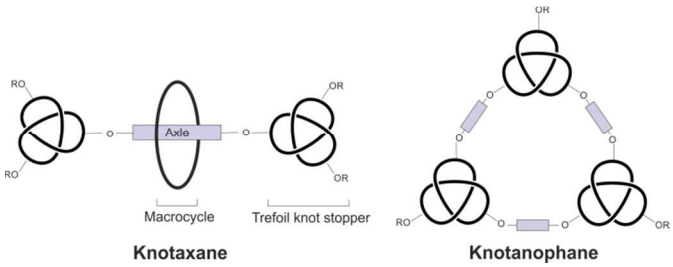

Figure 9: Schematic representations of two types of structures containing multiple knots.

More generally, once molecular knots have been created, they can then be derivatised, either to allow for the synthesis of higher assemblies of knots (see Section 2.2) or to alter or study the properties of the system itself. For example, an amide-based trefoil knot has been mono, di- and tri-dendronised to form molecules known as "dendroknots".[11] These have a knotted, topologically chiral core with one, two or three dendritic side-arms at the periphery. The chirality of the central knot has been shown to have some effect on the preferred orientation of the propeller-like dendritic substituents. Moreover, this type of functionalisation has allowed simple molecular knots to be used as nano-sized scaffolds for a wide range of potential applications.[5]

2.2 Molecules Containing Multiple Knots

Once the synthesis of simple molecular knots was established, it became possible to include knotted moieties into larger molecular structures. In knot theory, non-trivial knots can be added to make a composite knot, where knot addition means placing the two knots side-by-side, removing a short segment from each knot and joining the free ends of one knot to those of the other. In a similar way, tied open-chain fragments have been combined experimentally by Sauvage and co-workers to make molecular composite knots.[12] Knots that cannot be constructed by such an addition are called prime knots, and it is this type of knot that we have been considering so far in this review.

In chemistry, multiple non-trivial knots can be appended to simpler molecular structures, although this does not make them composite knots in the mathematical sense. The steric bulk of appended knots allows them to function as stoppers in a rotaxane, for example, as in the trefoil-knot-stoppered rotaxane shown in Figure 9 described as a 'knotaxane' by the authors.[5]

Small cyclic oligomers of up to four units in size have been produced using trefoil knot motifs as building blocks.[5] These types of structure have been termed "knotanophanes" (see Figure 9) and exist in a number of diastereomeric forms as a result of the chirality of each knot (see Figure 1). However, the topological isomers have similar physical properties making separation and/or identification of such molecules an interesting challenge.

2.3 Molecular Links

There are several iconic links in mathematical knot theory (see Figure 4) and these links have also become enticing synthetic targets for chemists. However, unlike the trefoil, which was only synthesised for the first time in 1989, the simplest link, the Hopf link, has been known in synthetic chemistry for far longer. In 1960, Wasserman was able to create small amounts of two interlocked molecular rings using a statistical threading approach.[13] He named the product a catenane, from the Latin "*catena*", meaning chain. The preparation of these molecular Hopf links (termed [2]catenanes) became far more efficient with the use of self-assembly and templating techniques, in a

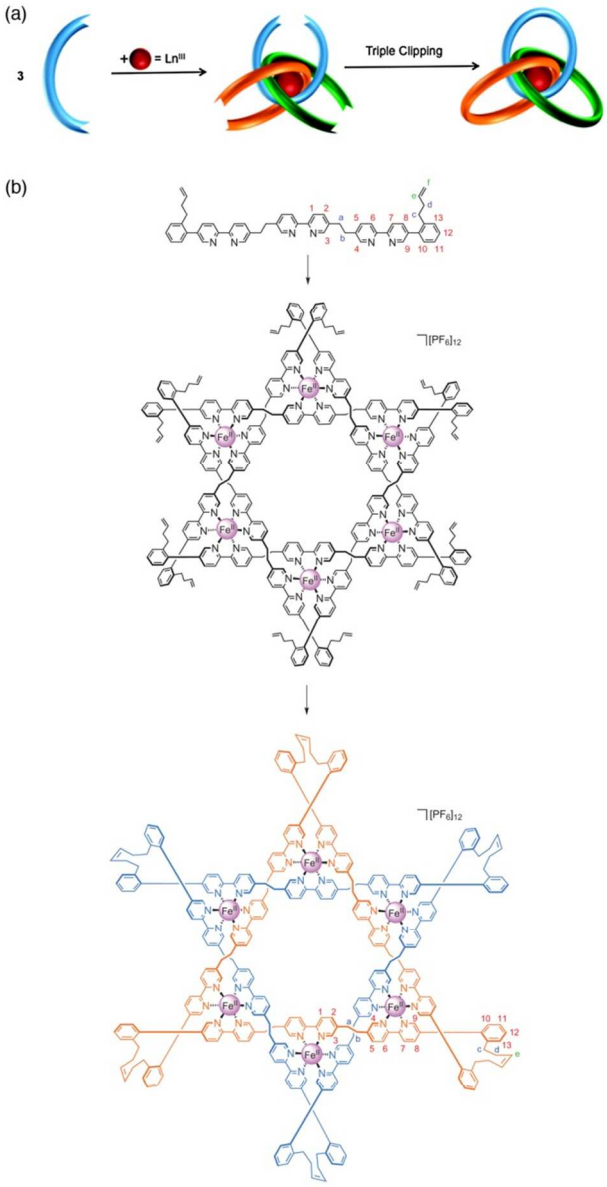

Figure 10: Synthetic strategies for a) Lanthanide-directed synthesis of a triply-interlocked [3]catenane involving a 1:3 metal to ligand ratio and self-assembly around the lanthanide (reproduced from Ref. 20 with permission from The Royal Society of Chemistry) and b) Star of David catenane involving six ligands which form a helicate structure around six Fe(II) cations (adapted with permission from Ref. 18).

similar way to the simple knots. In 1999, a method for producing [2]catenanes by using two pre-formed rings was reported and described as a molecular version of "magic rings".[14] The trick for achieving this interlocking was the introduction of metal ions into the ring backbone. Inclusion of these metals led to the formation of reversible metal-ligand bonds which allowed the pre-formed rings to split and reform once they became entwined with another.

The less common Solomon's link (sometimes less accurately called a Solomon's knot) can also be found in chemistry as a doubly-interlocked [2]catenane. Solomon's links, just like trefoil knots, are topologically chiral. The first successful synthesis of a molecular Solomon's link was achieved by using metal-templating to create a helical arrangement of molecular fragments which could then be cyclised to form the required doubly interlocked link.[15] Unfortunately, this only yielded approximately 2 % of the desired product. However, since then, several more efficient methods have been developed, such as "all-in-one" syntheses using template-directed self-assembly (Figures 8e and f).[16] On a similar theme, the so-called "Solomon's cube" was synthesised using a metallosupramolecular self-assembly process.[17] The Solomon's cube structure is essentially a Solomon's link motif involving four palladium ions and four tris(3-(3-pyridyl)phenylester)cyclotriguaiacylene ligands, of which the latter are able to intertwine producing the complex topology (Figure 8g).

One very recent example of synthetic advancement in this field is the preparation of a triply-interlocked [2]catenane, one which the authors called the Star of David catenane.[18] This procedure involved using six tris(2,2′-bipyridine) motifs which formed a helicate structure around six iron(II) cations. Ring-closing olefin metathesis then allowed for the final catenane formation. One of the key synthetic challenges in this development was the preparation of bipyridyl ligands which had restricted conformational space to force the olefin metathesis step to form the desired product rather than oligomers or cross-linked materials. Furthermore, the use of sulfate counterions was required to adjust the size of the circular helicate.

The first molecular Borromean rings (see Links, Section 1.2) were reported by the Stoddart group in 2004 (Figure 8d).[19] Since the Borromean rings are Brunnian, they are topologically distinct from triply-interlinked [3]catenanes like those in Figure 10, produced by the lanthanide-directed synthesis of Gunnlaugsson and co-workers; removal of one ring from the latter structure results in a Hopf link rather than the unlink.[20] As well as having fascinating mathematical properties, Borromean linkage motifs can also be found in a variety of materials (see Section 4.2).

2.4 Ravels

The term ravel, defined in the chemistry literature in 2008,[21] refers to a mathematical structure that has been studied for around forty years. It is a generalisation of a knot that allows three or more strands to fuse at a given point, known as a vertex. From a mathematical perspective we are now dealing

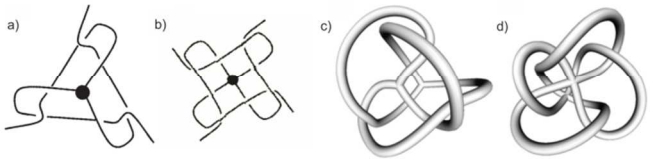

Figure 11: Symmetric representation of a) universal 3-ravel and b) universal 4-ravel and their corresponding minimally knotted graphs c) and d) obtained by joining all the loose ends of the ravel at an additional vertex. Adapted from Ref. 21 with permission from the Centre National de la Recherche Scientifique (CNRS) and The Royal Society of Chemistry.

with a graph in three-dimensional space, consisting of a collection of vertices together with a set of edges (the strands) that connect them. In graph theory, the term "valency" (or "degree") is used to refer to the number of edges connected to the vertex. An example of a graph with two trivalent vertices and three edges is shown in Figure 11c. A graph may contain cycles, which are closed loops obtained by following the edges of the graph from a starting vertex back to the same vertex without visiting any edge or intermediate vertex more than once. Graphs are perhaps most familiar in chemistry in the form of the bonding networks in molecules, where the vertices of the graph correspond to the atoms and the edges of the graph represent the chemical bonds.

A graph is called unknotted if it can be smoothly deformed (whilst avoiding edge intersections) to lie entirely within a plane. This definition for graphs is consistent with that for knots, since the only knot that can be deformed to lie entirely within a plane is the unknot; the planar projection of any other knot requires crossings that take strands out of the plane. One way to recognise that a graph is knotted (although this is not a necessary condition) is to identify a cycle in the graph that is a non-trivial knot. To go further and classify the specific topology of a graph, the concept of polynomial invariants for knots can be extended to graphs. For example, if two diagrams are merely different representations of the same graph, then they will have identical Yamada polynomials.[22] A particularly interesting family of graphs are those that are minimally knotted, which means that the graph is knotted even though all the cycles of the graph form only unknots or unlinks. One way to produce a minimally knotted graph is to take an unknotted graph and replace a vertex that has valency n with a universal n-ravel.[21] The universal 3-ravel and 4-ravel are displayed in Figure 11a and 11b and both have the property that joining all the loose ends to an additional vertex results in a graph (displayed in Figures 11c and 11d, respectively) that is knotted but contains only unknotted cycles and no links. These graphs are therefore simple examples of minimally knotted graphs. The crucial feature of a ravel is the mutual weaving of the edges that emerge from the single vertex, rather than any knotting or pairwise linking. In this respect, ravels are reminiscent of Brunnian links.

Recently, the first molecular ravel was synthesised by the Lindoy group which they described as like a "branched knot".[23] Twelve bis-β-diketone derivatives form a triple helicate structure with the use of ferric chloride to promote

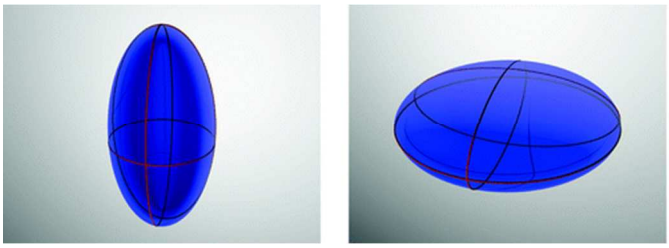

Figure 12: Examples of prolate (left) and oblate (right) ellipsoids. A prolate ellipsoid has the most circular equatorial ellipse perpendicular to the longest axis whereas an oblate ellipsoid has the shortest axis perpendicular to the most circular equatorial ellipse. The ellipsoids in this figure are equally aspherical. Reprinted with permission from Ref. 26. Copyright 2008 American Chemical Society.

metallosupramolecular self-assembly. The resultant self-interpenetrating architecture was shown (using X-ray diffraction) to be a universal 3-ravel (Figure 11c). It is proposed that non-covalent interactions such as π-π stacking contribute to the stability of the ravel structure along with efficient filling of space, making it more stable than the competing helicate. The successful realisation of such an intricately intertwined structure both represents a significant advance in synthetic control of molecular topology and opens up a range of new challenges for synthesis.

3. Polymers

The chain-like structure of a polymer makes it a potential host for knots. In this section, we examine the effects of knots on the physical properties of polymers.

3.1 Ring polymers

The natural conformation of a stiff, unbranched, linear polymer would be rod-like. Such structures, which are non-spherical and extend significantly further in one direction than in the two orthogonal directions, are called prolate. The opposite case, where the object is notably shorter in one direction than in the other two, is an oblate, disc-like structure (see Figure 12). It is well established, but not intuitively obvious, that even a completely flexible linear polymer is more likely to adopt a prolate than an oblate conformation at a given instant.[24] The origin of this result is entropic; there are more ways to arrange a freely jointed chain such that it defines a prolate shape than an oblate one.

A very stiff ring polymer, on the other hand, would have to adopt an oblate, circular configuration to minimise bending. Hence, it is even more surprising that, like linear polymers, a sufficiently flexible ring polymer is prolate on average.[25] However, a given ring polymer may only explore conformations that do not alter its topology. Rawdon *et al.* have investigated how the presence of a knot affects the average shape of flexible ring polymers by modelling them as freely jointed polygons of rigid struts.[26] The general effect of a knot is to make the conformations of the polymer more compact and less prolate than an unknotted polymer with the same number of segments. For a sufficiently small number of segments (6 or 8), it is even possible for the average shape of a trefoil knot to be oblate. The non-trivial topology places severe constraints on the conformations that can be explored by a hexagon or octagon, but polygons with a larger number of edges rapidly revert to being prolate on average. Figure 13 shows example conformations of a trefoil in a 50-segment chain. The shapes of the chain have been characterised in the images by their inertial ellipsoids, which show the extent to which the polymer's mass (carried by the vertices of the polygon) is distributed in three orthogonal directions.

In the case of circular DNA strands, the average size and shape has a strong influence on the molecules' mobility in electrophoresis. This technique uses a uniform electric field to pull the molecule through a gel against the friction caused by the gel network. Electrophoresis can separate topoisomers (molecules that differ by their knotting, linking or supercoiling) because they experience different frictional forces and therefore reach different drift velocities in a field of given strength. In low-density gels, the mobility of a given DNA strand increases with increasing knot complexity. This is because a given polymer becomes, on average, more compact with the complexity of the knot and can move through the gel more easily. However, in denser gels, the mobility initially decreases with increasing knot complexity and only starts increasing for still more complex knots.[27] One possible explanation for this non-monotonic behaviour is that more complex knots are not only smaller, but also less compressible because more complex knots are able to access fewer geometrical conformations for a given length of DNA. Hence, a less complex knot, though larger at equilibrium, can more easily deform to pass through a fine gel mesh. Sufficiently complex knots, however, would eventually be compact enough for the mobility to start increasing again.[27]

Simulations by Michieletto *et al.* suggest another possible explanation for the electrophoresis results.[28] Modelling the gel as an imperfect cubic mesh, where some of the edges were cut, these authors examined the effect of knots becoming impaled on the dangling ends of the gel. Although more complex knots were less likely to become impaled (due to their compactness), their entanglement was more likely to be severe, resulting in a longer delay before the molecule could resume its drift and causing an overall decrease in mobility.

3.2 Open polymers

Despite the fact that the mathematical definition of a knot only

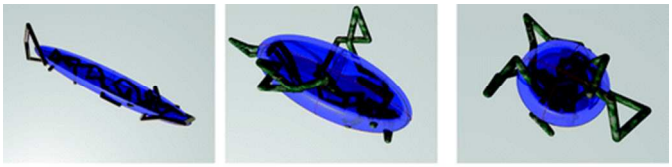

Figure 13: Three conformations of a 50-edge polygonal trefoil knot along with the corresponding inertial ellipsoid. The conformations are less prolate, more compact and more spherical going from left to right. Reprinted with permission from Ref. 26. Copyright 2008 American Chemical Society.

strictly applies to a closed loop, in everyday life we often refer to knots in open chains, such as shoelaces or electrical cables. An apparent knot in the middle of an extended string can intuitively be formalised by joining the ends of the string. However, if the ends are buried within the tangle (as always seems to be the case with Christmas tree lights) then there may be several ways to join the ends, making the topology of the knot ambiguous.

The same considerations come into play for knots in linear polymers, and several loop closure schemes have been developed.[29] A method for locating knots in protein chains was introduced by Taylor and led to the first detection (in protein structures that were already known) of a deeply embedded trefoil and the more complex figure-eight knot.[30] Taylor's method was to keep the ends of the chain fixed while notionally tightening the structure until it either collapses into a straight line (in the case of the unknot) or leaves a compact, well defined knot away from the ends. The tightening works by iteratively changing the position of each point on the chain to lie more in line with its immediate neighbours either side, subject to segments not passing through each other. However, this approach does not always lead to sufficient simplification because the tightening moves can become jammed.

An alternative method is to join the chain ends to arbitrary points that lie far outside the chain and to connect these extended end-points directly.[29] The topology of the closed loop can depend on the choice of external points, and statistical information can be gathered on how frequently a given knot is produced for random points. If no single result dominates this sampling, one may draw the valid conclusion that the topology is ambiguous. The disadvantage of such stochastic closure schemes is that repeated sampling of the knot type can be computationally costly.

An attractive method called the minimally interfering closure selects the path for connecting the chain ends depending on the structure itself.[31] This scheme starts by constructing the structure's convex hull, which is the smallest polyhedron that contains the structure and has no concave region on its surface. If the ends of the chain lie closer to each other than to the surface of the convex hull then the chain is closed by joining the ends directly with a straight line. If, instead, the ends lie closer to the hull, then they are extended through the closest points on the hull and joined externally. The minimally interfering closure usually returns the same result as the dominant knot found by stochastic closure, providing a reliable classification relatively efficiently.

The presence of a knot in a chain-like molecule can reduce its mechanical strength. Just as stretching a string with a knot results in rupture near the point where the string enters the tightened knot, stretching a knotted polymer first concentrates the strain energy in bonds at the entrance and exit of the knotted region and then leads to bond-breaking. This effect in molecules was first shown computationally[32] in a knotted alkane with Car-Parrinello molecular dynamics simulations, which use density functional theory to calculate the energy of the system and allow for bond breaking. The knotted alkane broke at a strain energy more than 20% lower than the unknotted chain. The weakening of the chain is associated with the high curvature in the knotted region. Stiff actin filaments are dramatically weakened by the presence of a knot, as shown in the experiments of Arai *et al.*[33] These authors tied knots in actin by attaching myosin-coated polystyrene bends to the ends of the filament and manipulating the beads using optical tweezers (see Figure 14). While a straight actin filament is able to withstand a tensile force of around 600 pN, the knotted filaments broke (near the knotted region) at less than 1 pN.[33]

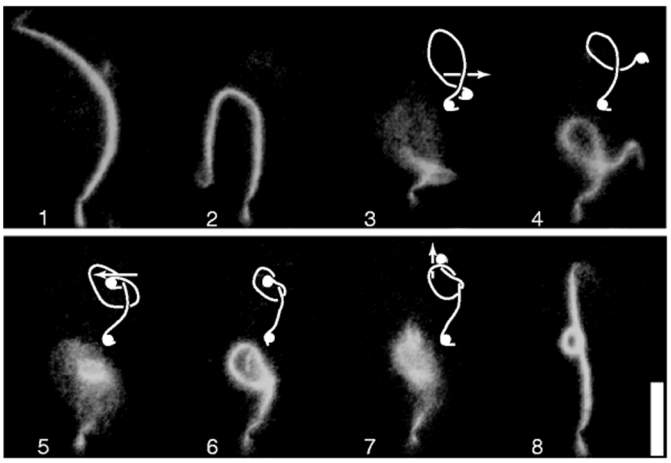

Figure 14: Tying a knot in an actin filament. Drawings overlaid on images 3-7 highlight the process occurring at each step. Reprinted by permission from Macmillan Publishers Ltd: Nature Ref. 33, copyright 1999.

The stiffness of a chain also affects the thermodynamics of knot formation. A stiff molecule must pay a high enthalpic penalty to be bent into a knot. In contrast, for a very floppy chain, the thermodynamic cost of a knot is largely entropic because the segments cannot pass through each other and the fixed topology therefore places a restriction on the conformations that the molecule can access by thermal fluctuations. In fact, recent simulations show that flexible chains can, on average, be less bent in the knotted region than their unknotted counterparts.[34] The net result is that there is a non-zero optimal stiffness at which the free energy of knot formation is minimised. This optimum seems to be independent of the knot type, but is shifted to lower stiffness if the chain is confined, since confinement reduces conformational entropy even in the absence of a knot.[34]

An important case of knot confinement concerns the DNA contained in the protein shell of a virus. The virus must expel genetic material in order to replicate, and the ejection process is strongly affected by the presence of knots. Simulations using a simple bead-and-spring model of DNA suggest that a knot acts as a ratchet during ejection through a pore.[35] The knot blocks ejection when it is pulled against the opening and the chain must reptate through the knot to make progress. However, if the knot diffuses along the chain into the interior of the capsid then unhindered ejection may resume. Hence, the process occurs in jerks with more complex knots resulting in slower ejection. More recent simulations show that the hindrance

caused by knots in the ejection process is greatly reduced if the tendency of DNA strands to align at a slight angle is accounted for.[36] These "cholesteric" interactions favour spooled, rather than randomly tangled conformations of the DNA within the virus. However, if the axis of the spool is not aligned with the opening in the shell then ejection will be delayed until the spool has rotated into a compatible orientation.

4. Network Materials

4.1 Coordination and supramolecular networks

So far we have considered knots in isolated molecules. However, knotted motifs can also be repeated to create a periodic, interwoven network. The field of topologically non-trivial coordination polymer networks is vast and has been comprehensively reviewed.[37] All interpenetrating network structures can be regarded as infinite, ordered polycatenanes or polyrotaxanes and can be classified by the dimensionality (0-D to 3-D) of the chemically bonded components that are linked together, and by the number, *n*, of independent interpenetrating networks. Trivially, a 0-D network consists of individual molecules ("zero-dimensional" components) such as macrocycles, which can be linked together, rather like paper chains, into a chain (1-D), sheet (2-D) or three-dimensional array. Such molecular linkages are not technically interpenetrated networks because the components are discrete. A recent example is an infinite [*n*]catenane comprising a copper(II) chloride metallomacrocycle with bridging phenanthrene-based imidazole ligands (Figure 15a).[38] 1-D coordination polymer chains can give rise to 1-D or 2-D interpenetrated networks, but a 3-D network based on 1-D components is not currently known. A 1-D polyrotaxane based on a silver(I) bis(imidazole) is shown schematically in Fig. 15b.

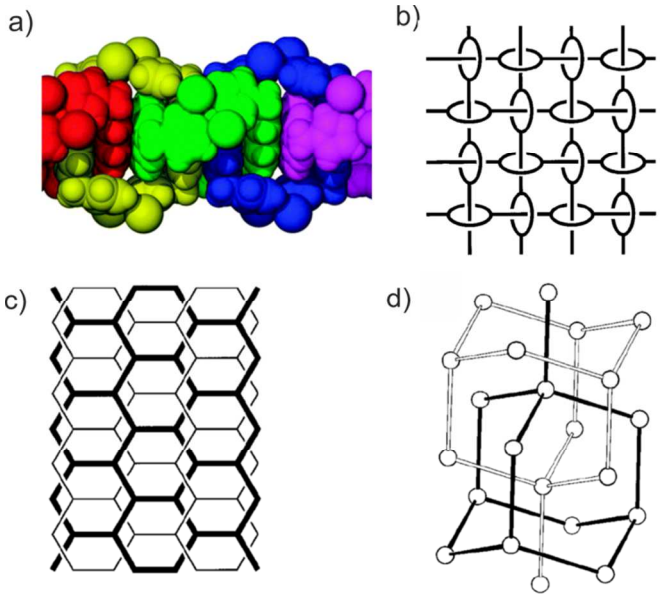

Figure 15: a) An infinite [*n*]catenane (adapted with permission from Ref. 38). b) A 1-D polyrotaxane. c) An example of a parallel interpenetrated net. d) An example of a diamondoid net. (b-d adapted with permission from Ref. 40)

1-D coordination polymers can also exhibit braided type structures[39] which, conceptually, can be derived from breaking the three discrete rings of a Borromean structure and extending the resulting linear threads to give a triple stranded braid. 2-D networks can form interpenetrated, polycatenated or Borromean type entanglements.[37] By far the most common are the polycatenated honeycomb and sql type (Shubnikov tetragonal plane) nets. An example of the honeycomb network is [Ag(tricyanomethanide)] which adopts one of four topologically different modes of parallel interpenetration, Fig. 15c. 3-D networks can adopt a wide variety of complex structure types, the most common being the diamondoid net, Fig. 15d, as exemplified by the twofold-interpenetrated $[Zn(CN)_2]$. The analysis of a network topology has been greatly facilitated in recent years by the ToposPro software which enables automated analysis and structure type assignment.[40] Network solids have a fascinating range of properties. For example, in some cases interpenetration can enhance the surface area of metal-organic frameworks resulting in enhanced gas sorption properties. In a different area, in 1993, a novel compound consisting of two fully interlocked graphite-like networks was found to exhibit magnetic properties below 22.5 K.[41] Designing such molecular magnets is a key challenge in materials science. The compound has the formula $(rad)_2Mn_2[Cu(opba)]_3(DMSO)_2{\cdot}H_2O$, where rad refers to 2-(4-*N*-methylpyridinium)-4,4,5,5-tetramethylimidazoline-1-oxyl-3-oxide and opba to orthophenylenebis(oxamato). The interlinking produces Hopf link type relationships between the two networks.

4.2 Gels

Knots are not a concept traditionally associated with gel structures. This is primarily because of the nature of the gel network, which comprises an extended sample-spanning mesh of fibres, few of which ever undergo closure. This means that knots, by their strict mathematical definition, are rarely formed. However, the fibres are susceptible to tangling, which locks them into a particular topological state just as a knot is defined by the crossings of a single closed curve. The tangling has a huge impact on the gel properties and behaviour, not least in supporting the permanent network that give gels their solid-like elastic properties despite comprising generally around 99%

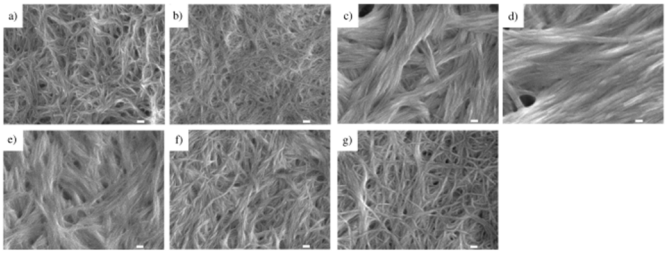

Figure 16: SEM images showing the effect of different molar ratios of L,L,L and D,D,D dendritic peptides on gel morphology. a) [L,L,L]=10 mM, [D,D,D]=0 mM; b) [L,L,L]=8.7 mM, [D,D,D]=1.3 mM; c) [L,L,L]=6.2 mM, [D,D,D]=3.8 mM; d) [L,L,L]=5 mM, [D,D,D]=5 mM; e) [L,L,L]=3.8 mM, [D,D,D]=6.2 mM; f) [L,L,L]=2.5 mM, [D,D,D]=7.5 mM; g) [L,L,L]=0 mM, [D,D,D]=10 mM. The white bar represents a distance of 100 nm. Reproduced with permission from 44.

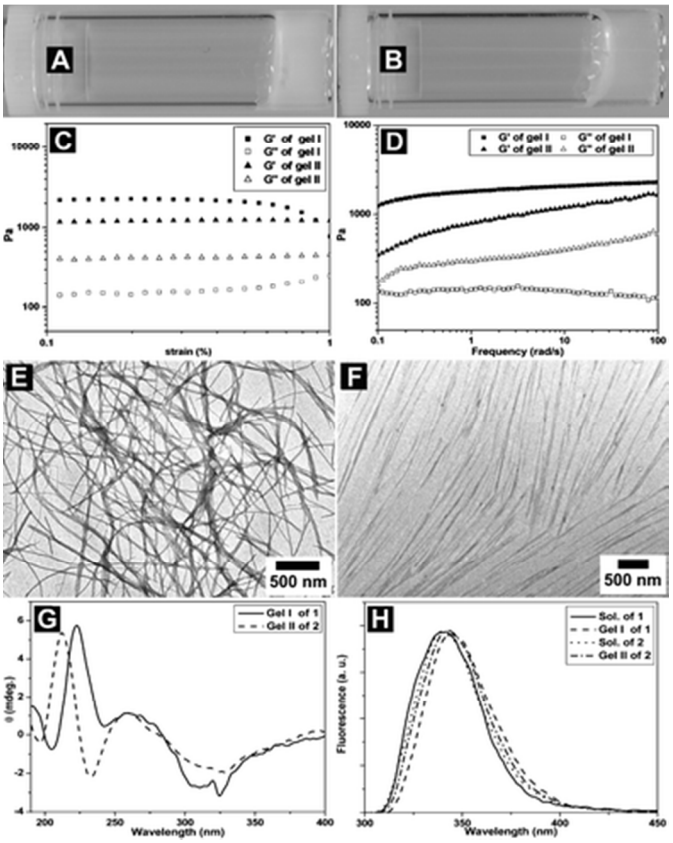

Figure 17: Optical images of A) Gel **I** and B) Gel **II**, C) strain and D) frequency dependence of dynamic storage moduli (G') and loss moduli (G'') of the hydrogels, TEM images of E) Gel **I** and F) Gel **II**, G) the CD spectra of the hydrogels and H) the emission spectra of both hydrogelators **1** and **2** in solution and in the hydrogels. Reproduced from Ref. 45 with permission from The Royal Society of Chemistry.

fluid. It has been shown that the mechanical properties of small-molecule gel systems do not match those of a colloidal gel.[42] Instead a more appropriate model is that of a cellular solid which is formed from interconnected load-bearing struts. The crosslinking of such structures allows the formation of tangled or knotted networks.

Ultra-strong chemical fibres are sometimes produced by orientational crystallisation from a gel medium.[43] Such fibres are grown with a fibrillar crystallite structure which gives them their strength. This requires the use of a supercooled, tangled gel network. Molecular tangles within this gel have been shown to be vital for the crystallisation process in this type of technique.

The degree of gel network entanglement has also been shown to be a key component in determining the morphology and macroscopic behaviour of two-component dendritic peptide gels.[44] Diaminododecane formed dumbell-like supramolecular complexes by hydrogen bonding with dendritic peptides incorporating three chiral centres, which gel toluene. Interestingly, the micro structures of the gels depended upon the relative configurations of the asymmetric carbon atoms in the peptides. Enantiomeric (L, L, L or D, D, D) gelator units were found to form highly fibrous structures whereas racemic gels (50 % L: 50% D) formed a flatter, more "woven" structure (see Figure 16). Gelator units based on a 1:2 ratio of L:D or D:L formed a fibrous assembly similar to the enantiomeric form but with significant changes when studied by small-angle X-ray scattering. These latter gels were also found to have reduced macroscopic stability compared to the pure enantiomeric version. The study also showed that the gelation behaviour of the L, D, D and D, L, L organogels was based on both the fibre helicity as well as their degree of entanglement.

Another example of stereochemistry affecting gel properties appears in work using D-glucosamine-based supramolecular hydrogels as a biomaterial to promote wound healing.[45] Two different gels were produced, one with Nap-L-Phe-D-glucosamine (Gel **I**) as the gelator and the other with Nap-D-Phe-D-glucosamine (Gel **II**). Both form stable hydrogels easily but the transmission electron micrograph (TEM) images of each show very different structures (shown in Figure 17). While Gel **I** is a tangled network of small, irregular ribbon bundles (Figure 17 E), Gel **II** comprises small, rigid ribbons with much more uniform widths and a far more ordered network (Figure 17 F). The various physicochemical properties of the two gels were studied and key differences between the circular dichroism (CD) spectra and rheological properties were noted.

While knots by the mathematical definition are not currently considered in gel materials, entanglement around nodes and amid the fibres is key and has many of the same mathematical characteristics as knots and braids.

5 Knots in Liquid Crystals

The knots described so far have all taken the form of particles that are joined to make a self-contained physical structure. However, it is also possible to create knots by disrupting the otherwise regular order of a background medium. Such knots are not a structure made out of particles that have been joined together but, rather, a defect that traces a path through a host material.

To visualise the concept, consider a nematic liquid crystal, consisting of rod-like molecules that are, on average, aligned in a particular direction so that there is long-ranged orientational order but only short-ranged, liquid-like correlation of the

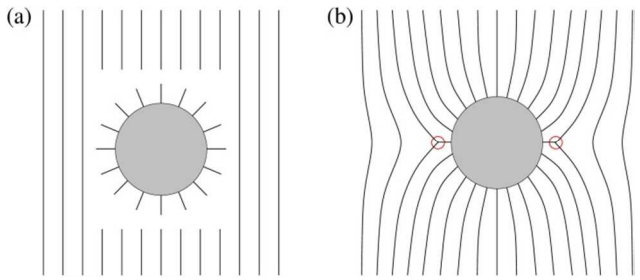

Figure 18: (a) The parallel lines of the director in a nematic liquid crystal are disrupted by the presence of a spherical colloid with perpendicular surface anchoring. (b) One topological solution is a disclination defect encircling the colloid in a plane perpendicular to the diagram, highlighted by the red circles in this cross section.

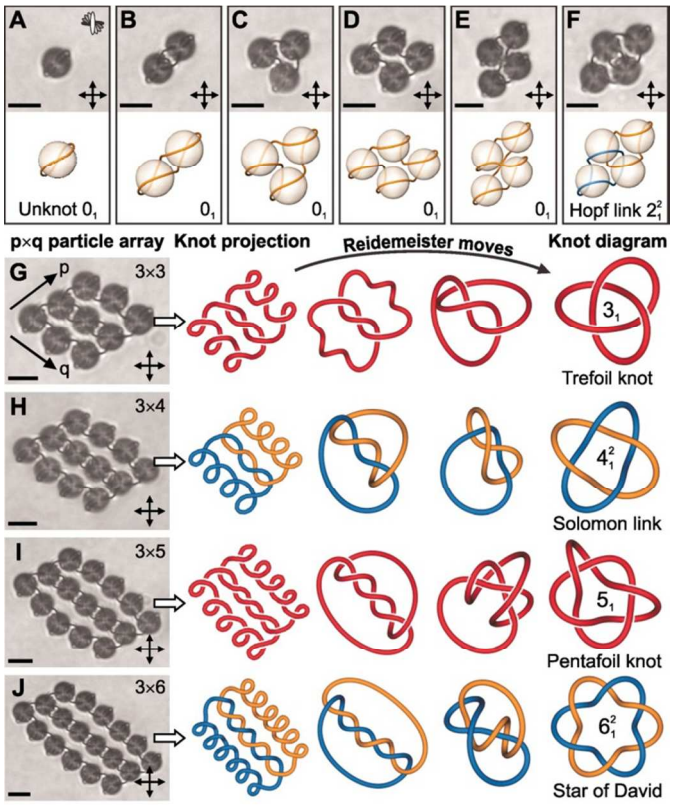

Figure 19: Colloidal spheres held together by disclination defects in a chiral nematic liquid crystal. A-E all show unknots formed by defect loops. F-J all show non-trivial knots and links. For G-J, the schematic diagrams show deformations that simplify the structure to the conventional representation of the relevant knots. In the optical images, the molecular orientation of the liquid crystal is aligned with crossed polarisers above and below the sample. The scale bars are 5 μm. From Ref. 46. Adapted with permission from AAAS.

molecules' positions. The average direction of the molecular axes can be represented by parallel lines running through the material. Introducing a spherical colloidal particle disrupts this alignment because the parallel lines cannot penetrate the colloid. Furthermore, the colloid may have a preference for the molecules of the liquid crystal to be anchored to its surface in a particular orientation. Figure 18a shows a cross-section through a spherical colloid with homeotropic (perpendicular) anchoring of the liquid crystal molecules. This local arrangement is incompatible with the background nematic ordering. One solution to the mismatch is the formation of a disclination defect,[46] consisting of a line at which three molecular alignments collide, as shown in Figure 18b. This defect encircles the colloid, forming a closed loop like a Saturn ring. The defects are readily visible under optical microscopy due to the strong scattering of the polarised light by the disordered regions of the liquid crystal, which makes them appear dark between crossed polarisers.

Being a defect in the nematic order, the disclination loop comes with a free energy cost. There is, therefore, a thermodynamic driving force to shorten the loop, and this causes the Saturn ring to act like a stretched elastic band that seeks to reduce its length by contracting. Nevertheless, because of the fixed topology imposed by the presence of the colloid, the defect cannot vanish altogether.

A pair of colloidal spheres can lower their combined free energy by allowing the regions of distorted liquid crystal that surround them to overlap, thereby reducing the overall distortion. Hence, the topological defects induce an effective attraction between the colloids, and the symmetry of the interaction is the same as that between two quadrupolar charge distributions.

It is also possible for the Saturn rings to join into a single disclination loop that entangles both particles, providing a mechanism for building structures out of the colloids, held together by the topological defect (Figure 19). In principle, defects may also become intertwined with themselves and with each other. A breakthrough in the practical realisation of this possibility came with the deployment of chiral nematic liquid crystals.[46] In a simple nematic, the molecules are, on average, oriented in a particular direction (called the director), which is the same at all points in the sample. In a chiral nematic, the direction of molecular alignment gradually rotates as one travels along an axis perpendicular to the director. This rotation results in twisted orientational order that has helical chirality, like a corkscrew. Disclination defects in a twisted nematic tend to be longer than in a simple nematic because they no longer lie in a plane, and this in turn encourages entanglement.

The topology of the defects can be manipulated using precisely focused laser tweezers to break them and reconnect them in a different way. This can be done at a "tangle", which is the region where two segments of the defect approach closely. The two segments each have two ends, which form the four vertices of a tetrahedron. There are three ways of directly connecting pairs of vertices in a tetrahedron, and these arrangements can be interconverted by cutting the segments with the laser and reorienting the liquid crystal director field to re-knot the tangle. In a trefoil knot, for example, any of the three crossings can be rewired to reverse the orientation of the crossing (resulting in an unknot) or to bypass the crossing altogether (resulting in a Hopf link). By a sequence of such operations, any desired topology can be made to order.[46]

The richness of defect structures is further enhanced if the spherical colloid is replaced by a particle that itself has more complex topology. For example, a colloid in the shape of a Möbius strip (with homeotropic anchoring on its broad surface) introduces new constraints due to the non-orientability of the surface (Figure 6). The disclination defect induced by such a particle must thread the hole in the Möbius strip and cannot be shrunk to a point.[47] However, the form that a defect adopts is also influenced by its free energy in the given liquid crystal medium. In the case of a multiply-twisted Möbius colloid, multiple small disclination loops that thread the strip may be more stable than a single defect that twists round the strip to make a torus knot[47] (see Section 6 and Figure 23).

In a recent development, micrometre-scale particles that themselves are knot-shaped have been used to induce defects in nematic fields[48] (Figure 20). The particles are polymeric tubes, created by a photopolymerisation process using spatially

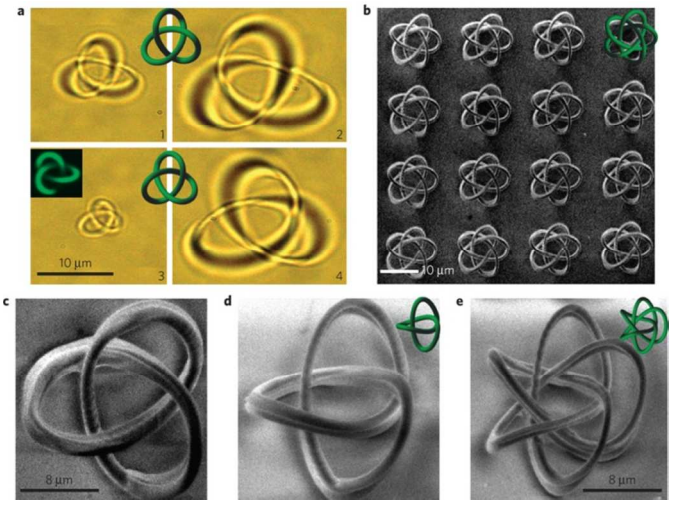

Figure 20: a) Optical micrographs showing photopolymerised colloidal trefoil knots, both left- (panels 1&2) and right-handed (panels 3&4), with corresponding models shown in green. b) Scanning electron micrograph of a 4×4 array of pentafoil knots on a glass substrate. c-e) Zoomed-in scanning electron micrographs of single knots with corresponding models shown in green. c) and d) are the same trefoil knot from different perspectives while e) is a pentafoil knot. Reprinted by permission from Macmillan Publishers Ltd: Nature Materials Ref. 48, copyright 2014.

patterned femtosecond laser pulses. The surface chemistry of these particles can be changed to switch the anchoring orientation of the liquid crystal between homeotropic (perpendicular) and tangential, which in turn changes the topology of the resulting defects. As for spherical colloids, the defects induce tuneable interactions between the knot-shaped microparticles. Martinez *et al.* [48] point out that these systems of interacting knots come rather close to a microscale realisation of Kelvin's vision of atoms as knots in the aether.[2]

In this introduction to knots in liquid crystals, we have concentrated on the topology of the defect lines. However, the molecular alignment in the regions between the defects is also important. In knot theory, the space around a knot (i.e., everything apart from the knot) is called the knot complement. In liquid crystals, the topology of a knotted defect does not completely determine the field of molecular alignment in the complement, so it is possible for two knotted defects with the same topology to have topologically different liquid crystalline "textures" around them.

6 Self-assembly of macromolecular and colloidal knots

We have now seen that molecular knots may arise by chance in long polymers, be built by careful synthetic procedures, or can even be tied mechanically using optical tweezers. However, some of the synthetic knots described in Section 2 can be regarded as forming by self-assembly in the sense that the components organise into a specific topology and structure without detailed external intervention. For any structure to self-assemble spontaneously, there must be a free energetic driving force from the unassembled components to the target structure. This driving force often involves a delicate interplay between enthalpic and entropic contributions, which must originate from the physical properties of the individual components, the interactions between them and the influence of the surrounding medium. Through the process of evolution, nature has developed many remarkable examples of complex self-assembly, including self-assembling knots in the form of proteins with a knotted native conformation.[7]

A protein is a linear polymer of amino acids, of which there are 20 types. The sequence of amino acids ultimately determines the compact folded structure that a protein adopts in its native state, and this structure is essential for the protein to perform its biological function. The most common protein knot is the trefoil, but knots as complex as 6_1 exist. There are also many examples of slipknots, *i.e.*, a threaded loop that is untied (rather than tightened) if the ends of the chain are pulled, like the bow of a shoelace. The existence of knotted proteins raises a number of interesting but difficult questions concerning the effect of the knot on physical properties of the protein, the evolutionary advantage of the knot, and the mechanism by which the knot is tied. The current state of knowledge in all these areas is included in the comprehensive recent review by Lim and Jackson.[7] Here we focus on ways that macromolecular systems can be designed to self-assemble into knots, and how some of the principles of self-assembly can be transferred to colloidal systems.

Proteins are distinguished from homopolymers, and from each other, by having a particular sequence of amino acid monomers. The addition of sequence information to the chain immediately provides a large degree of control over the structures that the chain adopts. Even a simple "HP" lattice model of proteins allows the likelihood of a nontrivial knot to be tuned from 10% to nearly 90% (see Figure 21).[49] In this model, each amino acid is represented by a single bead of just

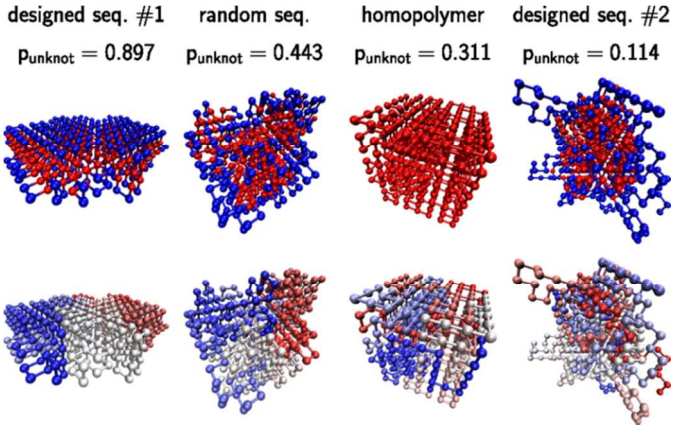

Figure 21: Representative native structures of a two-bead lattice protein and their probabilities p_{unknot} of the sequence adopting an unknotted structure. Designed sequence #1 displays almost no knots, the random sequence displays a moderate degree of knottedness, the homopolymer has a compact ground state but little local order internally, and the structure and designed sequence #2 is highly knotted. Upper row: hydrophobic monomers in red and polar monomers in blue. Lower row: chains coloured with blue monomers at the beginning of the sequence, changing to white in the centre and red at the end. Reprinted figure with permission from Ref. 49. Copyright 2015 by the American Physical Society.

two possible types (hydrophobic or polar) and is confined to a cubic grid of points. For real proteins with the variety offered by all 20 amino acids, there is evidence that a protein is less likely to be knotted than a homopolymer of the same length and flexibility, suggesting that evolution may have selected against knots in native states.[50]

Coluzza *et al.* have laid the groundwork for designing chains of colloidal particles that fold into a well-defined knotted conformation by mimicking certain features of proteins.[51] Their proposed "colloidal polymer" exploits existing technology for synthesising colloidal hard spheres with patchy interactions. Each patchy sphere has a single interaction site (the patch) that can form a reversible bond with that on another particle, imitating the interactions between amino acids due, for example, to hydrophobicity or to hydrogen-bonding. Chains of such particles can be designed to self-assemble into a selected knot in three stages. First, the structure and sequence of the chain must be explored together in a Monte Carlo simulation to identify plausible knotted structures. For a structure to be "designable" it must have a low energy for a large number of bead sequences. In the second stage, the chosen structure is held fixed while the sequence is optimised (by random mutations) to lower the energy. Finally, the designed sequence is tested by allowing the chain to fold in an unbiased simulation. Reinforcing the conclusion of Wüst, Reith and Virnau,[49] knotted ground states can be designed to fold reproducibly using only two types of bead (neutral and attractive), but the design protocol also works well with a 20-bead alphabet that mimics the natural amino acids.[51]

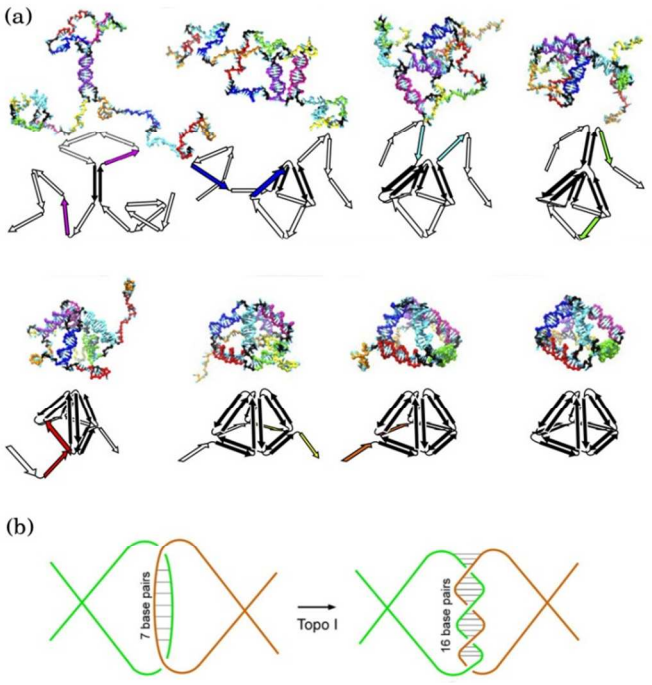

Figure 22: a) Self-assembly of a square pyramid from a single DNA strand that folds back on itself to hybridise into a double helix. The lower schematics highlight the segments that will hybridise in the next step, and the upper snapshots are taken from simulations of the assembly process. Adapted from Ref. 52. b) Topological alteration of kissing loops of single-stranded DNA into linked helices with increased base-pairing by the Topoisomerase I enzyme of *E. coli.* Adapted from Ref. 53.

The alphabet of interactions in DNA molecules is much smaller than that in proteins, with just four different nucleotides. However, the highly specific interactions in adenine-thymine and cytosine-guanine pairs make DNA a versatile macromolecule for self-assembly. Kočar *et al.* have used a combination of simulation and experiment to devise design rules for the efficient self-assembly of highly knotted DNA structures.[52] These authors took as their target a hollow square-based pyramid, in which each edge is a hybridised double helix of DNA. For a single DNA molecule to form such a structure, the strand must pass between the pyramid's five vertices on a route that travels along each edge exactly twice and in opposite directions (see Figure 22a). Although this underlying path is not knotted in itself, the final double helical structure requires the DNA strand to twist around itself. Once the initial edges of the pyramid have formed, this twisting can only be achieved by the termini of the strand repeatedly threading through the loops in the partially completed structure, generating a knot of around 30 crossings. For efficient folding, a "free-end rule" must be observed, where a free end is a segment of the DNA strand with no hybridised bases so far lying between it and the terminus. The rule states that each step in the self-assembly must involve at least one free end, which enables the strand to thread the existing loops relatively easily. Assembly is also assisted if hybridisation starts in the middle of the strand, and the long chains to either side of this section are both threaded early in the assembly process.

An alternative to building complex DNA knots that avoids repeatedly threading a chain end through a loop deploys enzymes to alter the topology of the assembly near crossings. Type I topoisomerases are naturally occurring enzymes that alter the linking number of double-stranded DNA complexes by cleaving one of the strands and reconnecting it on the opposite side of the other strand. In recent work, Seeman and coworkers have used Topoisomerase I from *Escherichia coli* to create knots and links from DNA.[53] Two complementary sections of single-stranded DNA are first brought together by "paranemic" cohesion i.e. where the strands lie side-by-side without being linked in a double helix. This partially frustrated arrangement allows some, but not all of the complementary pairs to cohere. The topoisomerase then acts at the kissing loops to cut one of the strands and reseal it so that they are linked, as shown in Figure 22b. The resulting double-helical structure enables full base-pairing between the complementary strands.

Both protein and DNA knots start with a chain that is eventually woven into a non-trivial topology. However, computational studies suggest that knots can also be self-assembled from fragments, with the underlying chain emerging at the same time as the knot. For example, knots have unexpectedly been found to be the ground state structures of certain Stockmayer clusters.[54] Stockmayer particles interact via a Lennard-Jones potential plus a point dipole and are an archetypal model for dipolar molecules or colloids that also have van der Waals attraction. The Lennard-Jones (van der Waals) interactions favour highly coordinated, compact

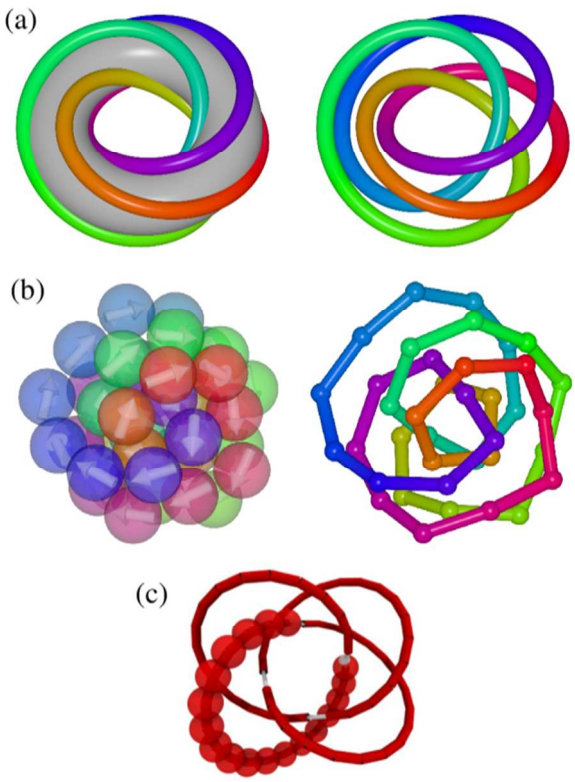

Figure 23: The 8_{19} torus knot a) idealised form with and without the toroidal surface, b) as the global potential energy minimum of a cluster of 38 Stockmayer particles represented as dipolar spheres (left) and balls-and-sticks (right), c) as self-assembled from helical templates (reproduced with permission from Ref. 55). In a) and b), the colour changes smoothly along the chain to help trace its path.

structures for small clusters, usually with icosahedral symmetry. In contrast, dipolar interactions favour a head-to-tail chain-like arrangement. The optimal compromise between these competing effects is sometimes a knot. The knot's underlying chain allows the dipole-dipole interactions to be largely satisfied, but twisting the chain and threading it through itself gives each particle more contacts than just its two neighbours in the chain, thereby satisfying the van der Waals attraction. Figure 23b shows an 8_{19} cluster that is the energetically optimal state of a 38-particle Stockmayer cluster. The 8_{19} knot was also found in self-assembly simulations of colloidal helical fragments that only interact through attractive sites at their tips, shown in Figure 23c.[55] The structures formed by such fragments can be tuned by adjusting their arc length and pitch. There is a remarkable coincidence between the knots found in this system and those that self-assembled from the Stockmayer particles.[54] The knots that emerge from the vast range of possible topologies are almost all torus knots. A torus knot is one that can be drawn by spiralling round a traditional holed doughnut two or more times before returning to the starting point, as illustrated in Figure 23a, the simplest, non-trivial torus knot being the trefoil. As the figure shows, the fact that torus knots can be drawn in such a regular way makes them rather special. Regularity can lead to efficient packing and interactions, in turn giving rise to the highly symmetrical self-assembled knots found in both the Stockmayer clusters[54] and the clusters of helical fragments.[55]

7 Conclusions

The demise of Kelvin's vortex theory of atoms in the late nineteenth century shifted interest in knots away from science and into the realm of pure mathematics. Over a century later, the resulting abstract theory of knots is being reunited with the physical sciences in ways that Kelvin could never have foreseen. The mathematical framework has been essential not only for identifying and classifying knots but, even more importantly, for helping to understand the physical consequences of knotted topology.

This tutorial review has touched on knot-related phenomena in the chemical sciences that are at different stages of their development. While basic catenane structures have been known for more than fifty years, it is only in the present decade that knotted defects in chiral nematics have been used to bind colloidal particles. Computer simulation is playing an increasingly important role in many of the fields, allowing the properties of knots to be tested systematically and predicted at a level of detail that is sometimes, but not always, experimentally accessible.

The present knot-related challenges in the chemical sciences are diverse but largely centre on understanding and then controlling the processes by which knots form. Such problems are often dynamic in character, so that knots are no longer the static, idealised drawings found in tables of knot topologies. We fully expect that knot theory and the chemical sciences will continue to intertwine in fascinating and sometimes unpredictable ways.

Acknowledgements

This work was supported by a Leverhulme Trust Research Programme Grant RP2013-K-009, Scientific Properties of Complex Knots (SPOCK).

Notes and references

[a] SPOCK Group, Department of Mathematical Sciences, Durham University, South Road, Durham, DH1 3LE, UK. Email: kate.horner2@durham.ac.uk; Tel: +44 (0)191 334 1510

[b] Department of Chemistry, Durham University, South Road, Durham, DH1 3LE, UK.

1 A. T. Vandermonde, *Memoires de l'Academie Royale des Sciences (Paris)*, 1771.

2 W. Thomson, *Philos. Mag. Ser. 4*, 1867, **34**, 15–24.

3 C. C. Adams, *The Knot Book*, American Mathematical Society, 2004.

4 G. R. Schaller and R. Herges, *Chem. Commun.*, 2013, **49**, 1254–1260.

5 O. Lukin and F. Vögtle, *Angew. Chem. Int. Ed.*, 2005, **44**, 1456–1477.

6 J.-F. Ayme, J. E. Beves, C. J. Campbell and D. A. Leigh, *Chem.*

Soc. Rev., 2013, **42**, 1700–1712.

7 N. C. H. Lim and S. E. Jackson, *J. Phys. Condens. Matter*, 2015, **27**, 354101.

8 C. O. Dietrich-Buchecker and J.-P. Sauvage, *Angew. Chem. Int. Ed.*, 1989, **28**, 189–192.

9 J.-F. Ayme, J. E. Beves, D. A. Leigh, R. T. McBurney, K. Rissanen and D. Schultz, *Nat. Chem.*, 2011, **4**, 15–20.

10 V. Marcos, A. J. Stephens, J. Jaramillo-Garcia, A. L. Nussbaumer, S. L. Woltering, A. Valero, J.-F. Lemmonnier, I. J. Vitorica-Yrezabal and D. A. Leigh, *Science*, 2016, **352**, 1555–1559.

11 J. Recker, W. M. Müller, U. Müller, T. Kubota, Y. Okamoto, M. Nieger and F. Vögtle, *Chem. Eur. J.*, 2002, **8**, 4434–4442.

12 R. F. Carina, C. Dietrich-Buchecker and J. P. Sauvage, *J. Am. Chem. Soc.*, 1996, **118**, 9110–9116.

13 E. Wasserman, *J. Am. Chem. Soc.*, 1960, **82**, 4433–4434.

14 M. Fujita, *Acc. Chem. Res.*, 1999, **32**, 53–61.

15 J. Nierengarten and C. Dietrich-Buchecker, *J. Am. Chem. Soc.*, 1994, **5**, 375–376.

16 R. S. Forgan, J.-P. Sauvage and J. F. Stoddart, *Chem. Rev.*, 2011, **111**, 5434–5464.

17 T. K. Ronson, J. Fisher, L. P. Harding, P. J. Rizkallah, J. E. Warren and M. J. Hardie, *Nat. Chem.*, 2009, **1**, 212–216.

18 D. A. Leigh, R. G. Pritchard and A. J. Stephens, *Nat. Chem.*, 2014, **6**, 978–982.

19 K. S. Chichak, S. J. Cantrill, A. R. Pease, S. Chiu, G. W. V Cave, J. L. Atwood and J. F. Stoddart, *Science*, 2004, **304**, 1308–1312.

20 C. Lincheneau, B. Jean-Denis and T. Gunnlaugsson, *Chem. Commun.*, 2014, **50**, 2857–2860.

21 T. Castle, M. E. Evans and S. T. Hyde, *New J. Chem.*, 2008, **32**, 1484–1492.

22 S. Yamada, *J. Graph Theory*, 1989, **13**, 537–551.

23 F. Li, J. K. Clegg, L. F. Lindoy, R. B. Macquart and G. V Meehan, *Nat. Commun.*, 2011, **2**, 205.

24 W. Kuhn, *Kolloid-Zeitschrifft*, 1934, **68**, 2.

25 K. Alim and E. Frey, *Phys. Rev. Lett.*, 2007, **99**, 1–4.

26 E. J. Rawdon, J. C. Kern, M. Piatek, P. Plunkett, A. Stasiak and K. Millett, *Macromolecules*, 2008, **41**, 8281–8287.

27 J. Cebrian, M. J. Kadomatsu-Hermosa, A. Castan, V. Martinez, C. Parra, M. J. Fernandez-Nestosa, C. Schaerer, M. L. Martinez-Robles, P. Hernandez, D. B. Krimer, A. Stasiak and J. B. Schvartzman, *Nucleic Acids Res.*, 2015, **43**, e24.

28 D. Michieletto, D. Marenduzzo and E. Orlandini, *Proc. Natl. Acad. Sci.*, 2015, **112**, E5471–E5477.

29 K. C. Millett, E. J. Rawdon, A. Stasiak and J. I. Sułkowska, *Biochem. Soc. Trans.*, 2013, **41**, 533–537.

30 W. R. Taylor, *Nature*, 2000, **406**, 916–919.

31 L. Tubiana, E. Orlandini and C. Micheletti, *Prog. Theor. Phys. Suppl.*, 2011, **191**, 192–204.

32 A. Saitta, P. Soper, E. Wasserman and M. Klein, *Nature*, 1999, **399**, 46–48.

33 Y. Arai, R. Yasuda, K. Akashi, Y. Harada, H. Miyata, K. Kinosita and H. Itoh, *Nature*, 1999, **399**, 446–448.

34 P. Poier, C. N. Likos and R. Matthews, *Macromolecules*, 2014, **47**, 3394–3400.

35 R. Matthews, A. A. Louis and J. M. Yeomans, *Phys. Rev. Lett.*, 2009, **102**, 088101.

36 D. Marenduzzo, C. Micheletti, E. Orlandini and D. W. Sumners, *Proc. Natl. Acad. Sci. USA*, 2013, **110**, 20081–20086.

37 L. Carlucci, G. Ciani, D. M. Proserpio, T. G. Mitina and V. A. Blatov, *Chem. Rev.*, 2014, **114**, 7557–7580.

38 L. Loots and L. J. Barbour, *Chem. Commun*, 2013, **49**, 671–673.

39 G.-P. Yang, L. Hou, X.-J. Luan, B. Wu and Y.-Y. Wang, *Chem. Soc. Rev.*, 2012, **41**, 6992–7000.

40 S. R. Batten and R. Robson, *Angew. Chem. Int. Ed.*, 1998, **37**, 1460–1494.

41 H. O. Stumpf, L. Ouahab, Y. Pei, D. Grandjean and O. Kahn, *Science*, 1993, **261**, 447–449.

42 C. E. Stanley, N. Clarke, K. M. Anderson, J. A. Elder, J. T. Lenthall and J. W. Steed, *Chem. Commun.*, 2006, **1**, 3199–3201.

43 P.-G. de Gennes, *Scaling Concepts in Polymer Physics*, Cornell University, 1979.

44 A. R. Hirst, D. K. Smith, M. C. Feiters and H. P. M. Geurts, *Chem. Eur. J.*, 2004, **10**, 5901–5910.

45 Z. Yang, G. Liang, M. Ma, A. S. Abbah, W. W. Lu and B. Xu, *Chem. Commun.*, 2007, 843–845.

46 U. Tkalec, M. Ravnik, S. Čopar, S. Žumer and I. Muševič, *Science*, 2011, **333**, 62–65.

47 T. Machon and G. P. Alexander, *Proc. Natl. Acad. Sci.*, 2013, **110**, 14174–14179.

48 A. Martinez, M. Ravnik, B. Lucero, R. Visvanathan, S. Zumer and I. I. Smalyukh, *Nat. Mater.*, 2014, **13**, 258–263.

49 T. Wüst, D. Reith and P. Virnau, *Phys. Rev. Lett.*, 2015, **114**, 028102.

50 R. C. Lua and A. Y. Grosberg, *PLoS Comput. Biol.*, 2006, **2**, 350–357.

51 I. Coluzza, P. D. J. Van Oostrum, B. Capone, E. Reimhult and C. Dellago, *Phys. Rev. Lett.*, 2013, **110**, 1–5.

52 V. Kočar, J. S. Schreck, S. Čeru, H. Gradišar, N. Bašić, T. Pisanski, J. P. K. Doye and R. Jerala, *Nat. Commun.*, 2016, **7**, 10803.

53 Y. P. Ohayon, R. Sha, O. Flint, A. R. Chandrasekaran, H. O. Abdallah, T. Wang, X. Wang, X. Zhang and N. C. Seeman, *ACS Nano*, 2015, **9**, 10296–10303.

54 M. A. Miller and D. J. Wales, *J. Phys. Chem. B*, 2005, **109**, 23109–23112.

55 G. Polles, D. Marenduzzo, E. Orlandini and C. Micheletti, *Nat. Commun.*, 2015, **6**, 6423.